Polarization transitions in interacting ring 1D arrays

Bahman Roostaei[1] and Kieran J. Mullen,[1]

[1]*Dept. of Phys. and Ast., University of Oklahoma, Norman,OK 73019*

(Dated: February 6, 2008)

Periodic nanostructures can display the dynamics of arrays of atoms while enabling the tuning of interactions in ways not normally possible in Nature. We examine one dimensional arrays of a "synthetic atom," a one dimensional ring with a nearest neighbor Coulomb interaction. We consider the classical limit first, finding that the singly charged rings possess antiferroelectric order at low temperatures when the charge is discrete, but that they do not order when the charge is treated as a continuous classical fluid. In the quantum limit Monte Carlo simulation suggests that the system undergoes a quantum phase transition as the interaction strength is increased. This is supported by mapping the system to the 1D transverse field Ising model. Finally we examine the effect of magnetic fields. We find that a magnetic field can alter the electrostatic phase transition producing a ferroelectric groundstate, solely through its effect of shifting the eigenenergies of the quantum problem.

PACS numbers: 73.21-b

I. INTRODUCTION

Fabrication of micro- and nano-sized structures such as quantum dots, wires and rings has made it possible for physicists to examine new ideas in electronic devices. These small size devices act as artificial atoms with spectra and shell structures similar to those of real atoms[1]. However it is possible to control the properties of these synthetic atoms in a way that is impossible with real ones. For example, a regular atomic orbital is three dimensional and one has limited control over the electronic wavefunction. In contrast, by controlling the shape of a quandum dot we can distort the wavefunction, controlling its polarizability and its interaction with adjacent dots. While the properties of periodic arrays of atoms are well understood in solid state physics, we have new playing field – periodic arrays of nanostructures – in which we have an unprecedented control of the "atomic states."

The focus of this paper is on the periodic one dimenstional (1D) arrays of nano-rings. We chose this system for two reasons. First, quantum rings display interesting phenomena (e.g. persistent currents[4, 5, 6, 7].) which are not found in dots. The basic difference between the ring geometry and a quantum dot is the excluded middle which confines the electron in a ring to a narrow spatially periodic channel. This compact, periodic geometry can allow dynamics not found in other systems.[8] Second, it has been become possible to create extremely small rings. These arrays of nano-rings can be fabricated either by dry etching [3] or by using MBE techniques to foster self assembled InGaAs/GaAs rings. The size of these nano-rings is ∼30 nm for outer radius and ∼10 nm for inner radius for self-assembled InGaAs/GaAs rings [2]. Such techniques not only produce extremely small rings, they also make it easy to make *periodic* arrays of small rings.

In this paper we consider an ideal array of 1D rings at zero temperature, each carrying a single charge. The rings are sufficiently close together that there is a Coulomb interaction between the electrons, but separated enough so that the tunneling between rings can be neglected,[9] as discussed in section II. In section III we consider the classical case in section and see how different assumptions allow for symmetric or symmetry breaking ground states. Section IV contains the main results of this work, where we show that there is a *quantum phase transition* in a 1D array of rings for $B = 0$. We show this both through Monte Carlo simulation of $1 + 1$D classical statistical respresentation of the problem as well as mapping it on to the 1D transverse field Ising model. The polarization pattern is antiferroelectric. In section V we examine how this transition is affected by magnetic fields. We conclude in section VI by summarizing results and discussing possible applications.

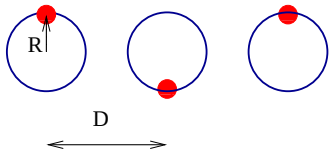

FIG. 1: A schematic picture of the groundstate of classical point electrons for 1D array of rings. The ring radius is R and the separation is D. The 1D ordering is antiferroelectric for the infinite size system and thus has a double degenerate groundstate.

II. THE MODEL

We consider a one dimensional array of singly charged narrow quantum rings with radius R and center-to-center separation of D (Fig.1). The width of each ring is much smaller than its inner radius so that we need only consider the one dimensional movement of the electron around the ring. While the rings are isolated from each other so there is no charge transfer between rings, the rings still interact electrostatically with their nearest neighbors.[9]

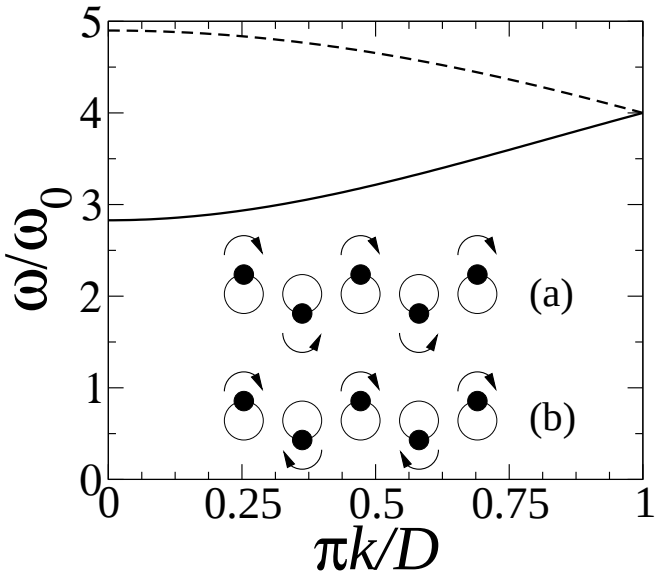

FIG. 2: Normal modes of the 1D ring array with gaps of (solid line, inset (a)) $2\sqrt{2}\omega_0$ and (dashed line, inset(b)) $2\sqrt{6}\omega_0$, where $\omega_0 = \sqrt{e^2/m^* D^3}$

While in principle the Coulomb interaction is long range, we assume that there is sufficient screening that next nearest neighbor interactions can be neglected.

We also neglect tunneling between rings. This is reasonable since the physical realizations discussed above produce rings that are not in tunneling contact. Tunneling will be exponentially suppressed with D, so that for spatially distinct rings it will be minimal.

All the phenomena explained in this article only will appear in experiments if the electrons do not lose their quantum mechanical phase, i.e. the ring's perimeter has to be smaller than the electron's coherence length ($2\pi R < L_\phi$) and the temperature has to be lower than the dephasing temperature ($T < T_\phi$).

In each ring the confinement energy of the electron scales as $E_q = \hbar^2/2m^*R^2$; this energy opposes localization of the wavefunction in the ring. The inter-ring Coulomb repulsion, which scales as $E_c = e^2/D$, tries to localize the wavefunction. Electrons are repelled from regions of the ring where it is too close to the charges on neighboring rings. The competition between these two physical scales creates a *quantum phase transition* in the array from a localized state to extended state as we will see below.

III. CLASSICAL RESULTS

Before solving a quantum mechanical problem it is often helpful to look at the similar classical case which is usually easier to solve. Below we consider two classical models, one in which the classical charges are treated as ideal points, and the second in which they are treated as a continuous fluid.

A. Classical point charges

The classical model considers one charged point particle per ring with only nearest neighbor Coulomb interaction. Unlike the quantum mechanical case there is only one energy scale in the classical problem which is the Coulomb energy $E_c = e^2/D$. The energy of a 1D array is given by $U_{1D} = \sum_{i=1}^{N} e^2/|\vec{r}_i(\theta_i) - \vec{r}_{i+1}(\theta_{i+1})|$, where θ_i is the location of the i-th electron as measured from horizontal axis. In the dipole approximation we can write this as :

$$\begin{aligned} U_{1D} - U_0 &\approx \frac{\epsilon^2 e^2}{2D} \sum_i [3\cos 2\theta_i + \cos(\theta_i - \theta_{i+1}) \\ &- 3\cos(\theta_i + \theta_{i+1})] \\ &= \frac{\epsilon^2 e^2}{D} \sum_i \left[\vec{s}_i \cdot \vec{s}_{i+1} + \frac{3}{2}(\hat{D} \cdot (\vec{s}_i - \vec{s}_{i+1}))^2 \right]. \end{aligned} \tag{1}$$

where $\epsilon \equiv R/D$ and U_0 is a constant, $U_0 \equiv \frac{Ne^2}{D}(1 + \frac{\epsilon^2}{2})$. In the second expression we identify the position of each charge by a vector $\vec{s}_i$ in the 2D plane pointing from the center of the i-th ring to the charge on that ring. The unit vector $\hat{D}$ lies on the horizontal axis.

The $\cos 2\theta$ (or $(\hat{D} \cdot \vec{s})^2$) term explicitly breaks the rotational symmetry, driving the system from XY to Ising-like behavior. The Heisenberg term in the last line of equation (1) drives the system ferroelectric at zero temperature while the second and larger term favors states where neighbors point in opposite direction. Thus the system at zero temperature orders in an antiferroelectric (AFE) pattern (Fig.1) in one dimension. Our numerical Monte Carlo simulations of the exact Coulomb interaction also verifies the existence of such a minimum energy configuration in the classical finite size arrays.

We can examine the stability of the AFE state by finding the higher energy modes of the system. We expand the energy function (1) to quadratic order in displacement angle around the AFE configuration using $\theta_i = (-1)^i \frac{\pi}{2} + \alpha_i$. The AFE configuration has a basis with two sites so we find two independent normal modes with frequencies :

$$\omega_{\pm}^{(1D)}(k) = 2\omega_0 \sqrt{4 \pm 2\cos\frac{kD}{2}}. \tag{2}$$

Where $\omega_0 \equiv \sqrt{e^2/m^*D^3}$. Both the modes are gapped since the Ising-like term provides the harmonic restoring force at each site. The modes are shown in Fig.(2). Normal modes are found to be independent of the ring radius.

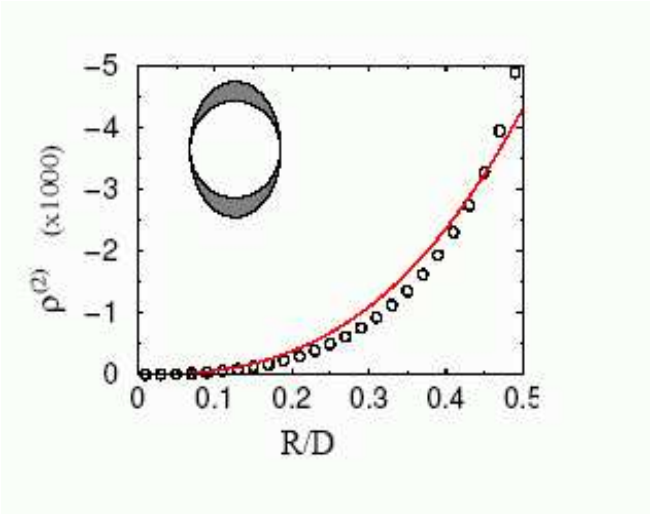

FIG. 3: A plot of the second fourier amplitude of the classical charge distribution on a ring in a 1D horizontal array. The circles are numerical results, the solid line is a scaled plot of eq.(4). Scaling is required since the analytic result neglects all higher fourier modes. Inset: a sketch of the charge distribution that corresponds to this Fourier mode. Note that the symmetry of the array is not broken by the charge distribution.

B. Classical charge fluid

Another interesting classical limit of our ring problem is when there is a classical *self-interacting* fluid of charge on each ring while the nearest neighbor fluids are still interacting with each other.

To find the minmum energy distribution of charge density on each ring we define an angular dependent charge density $\rho_i(\theta_i)$ on each ring where:$\int \rho_i(\theta_i)d\theta_i = 1$. We are looking for the minimal solution to the variational quantity :

$$I = \frac{1}{2}\int d\theta \int d\theta' \sum_{\langle ij\rangle} \frac{\rho_i(\theta)\rho_j(\theta')}{|\vec{r}_i - \vec{r}_j|} + \lambda \sum_i \int d\theta \rho_i(\theta). \quad (3)$$

For a 1D ring this expression is divergent due to self energy. We can regularize this in several ways. One method is to introduce a short distance cutoff ζ to the Coulomb interaction, discretize the integral equation and then solve the problem numerically. An approximate analytic solution can then be obtained by Fourier expanding the distribution, keeping only the first three modes.

For 1D array with periodic boundary condition we find that the amplitude of the non-trivial Fourier mode as a function of ζ and $\epsilon \equiv R/D$ for ρ is given by :

$$\hat{\rho}^{(2)} \approx \frac{-3\pi\epsilon^3(2-5\zeta^2)}{4(-2+4\log(\epsilon/\zeta))}. \quad (4)$$

We compare this analytic result with the numerical diagonalization of (3) in Fig.(3). As we can see in Fig.(3) the minimum energy configuration of the 1D array of charge fluid does not break the up-down symmetry of the system.

IV. QUANTUM RESULTS FOR $B = 0$.

At first glance the quantum mechanical wavefunction of a charged particle resembles the classical charge fluid. Although the wavefunction does not have a self-interaction, the quantum particle has a kinetic energy which opposes localization, making the analogy to charge fluid even stronger. Unlike the classical case, the quantum problem has two competing energy scales: the quantum kinetic energy, E_q, preventing localization and the Coulomb interaction energy, E_c, trying to force the charges away from each other. At $E_q \ll E_c$ we expect charge localization on each ring and at $E_q \gg E_c$ we expect no localization of charge. However it is not *a priori* obvious whether the charge localization (system polarization) breaks symmetry or not, whether this localization is a smooth function of the external parameters, and if it is a phase transition, what is the exact nature of this transition.

A. Variational calculation

As a first step we can use a simple variational wavefunction to find the polarization behavior of the system in ground state. The dimensionless hamiltonian of an array of one dimensional rings with radius R is given by:

$$\hat{H} = -\sum_i \frac{\partial^2}{\partial\theta_i^2} + \delta \sum_{\langle ij\rangle} \frac{1}{|\vec{r}_i(\theta_i) - \vec{r}_j(\theta_j)|}, \quad (5)$$

where $\delta = E_c/E_q$ is the interaction strength and the energy is measured in units of $E_q = \hbar^2/2mR^2$.

To find the ground state energy of the 1D array we employ a simple ansatz for the wavefunction of each sublattice : $\psi_A(\theta) = \frac{\sqrt{1-y^2}}{\sqrt{2\pi}} + \frac{y}{\sqrt{2\pi}}\cos(\theta-\phi)$ and $\psi_B(\theta) = \frac{\sqrt{1-y^2}}{\sqrt{2\pi}} - \frac{y}{\sqrt{2\pi}}\cos(\theta-\phi)$ alternately. The ground state values of y and ϕ is obtained by minimizing the energy (5) using dipole approximation for Coulomb interaction we find:

$$y(\delta,\epsilon) = \begin{cases} \frac{1}{4}\sqrt{11 - \frac{4}{\delta\epsilon^2}} & \text{for } \delta \geq \delta_c(\epsilon) \\ 0 & \delta < \delta_c(\epsilon) \end{cases} \quad (6)$$

and $\phi = \pi/2$, where the critical value of the interaction is given by $\delta_c(\epsilon) = \frac{4}{11}\epsilon^{-2}$. To find out the degree of polarization we define the *staggered polarization* vector as:

$$\vec{P}_s = \sum_i (-1)^i \int d\theta |\psi_i(\theta)|^2 \vec{r}_i(\theta). \quad (7)$$

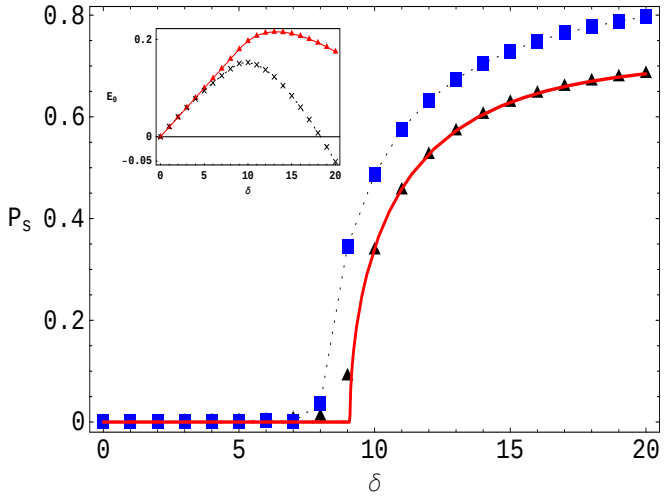

FIG. 4: A comparison of numerical and analytical calculations of the staggered polarization and energy as a function of δ in a 1D quantum ring array obtained in the Hartree approximation. The numerical results are for the case include Fourier modes $|m| \leq 1$ (triangles) and $|m| \leq 6$ (boxes). The solid line is the analytic result assum- ing $|m| \leq 1$. The quantity δ is a measure of the competition between the Coulomb interaction and the quantum kinetic energy

Using variational results the staggered polarization of the system is as follows:

$$\vec{P}_s(\delta,\epsilon) = \begin{cases} \frac{1}{8}\left(\frac{4+5\,\delta\epsilon^2}{2\delta\epsilon^2}\right)^{\frac{1}{2}}(11-\frac{4}{\delta\epsilon^2})^{\frac{1}{2}}\hat{D}_\perp & \delta \geq \delta_c \\ 0 & \delta \leq \delta_c \end{cases} . \quad (8)$$

Where $\hat{D}_\perp$ is the unit vector perpendicular to the common axis of the rings (Fig.1) and δ_c is defined in equation (6).

As we can see variational calculation suggests that the ground state of the 1D array of rings antiferroelecrically polarizes in perpendicular direction at high interaction strengthes while at lower values the wavefunctions are not localized, hence the system has no polarization. The validity of this result will be confirmed in next sections using more exact and reliable methods of calculation.

B. Hartree Approximation

The rings considered here are well separated with exactly one electron on each ring. Under this condition and because of strong Coulomb repulsion the effect of inter-ring transfer of electrons and overlap of wavefunctions is small. We can therefore neglect the inter-ring transfer from our calculations. Since without overlap the electrons do not have any exchange interaction, the Hartree approximation is exact for this problem.[10]

We can decompose the wavefunction in each ring into a limited number of Fourier modes, $\psi_i(\theta) = \sum_{n=-n_0}^{n_0} c_n e^{in\theta}$, and then solve the system numerically in the Hartree approximation. We impose the periodic boundary conditions on the array and by an iterative self-consistent method we find the ground state wavefunction of the rings. In Fig.(4) we can see the numerical results of the polarization and energy change of the 1D array of rings for different number of Fourier modes using exact Coulomb interaction and also its agreement with the variational calculation when we restrict the number of Fourier modes to $n \in \{-1, 0, 1\}$. The results are little changed when we increase the number of Fourier modes mostly in the high coupling regime.

All the above results suggest that there is transition from unpolarized to polarized state at zero temperature by changing the coupling. By looking at the behavior of polarization when the number of Fourier modes increases we realize that this transition tends to be sharper and sharper for higher number of Fourier modes suggesting a true phase transition in the system. If true, this transition would be a sudden change of ground state of the quantum system at zero temperature, known as *quantum phase transition*.[11] We demonstrate that this is the case and determine the universality class of the transition in the next section using the Monte Carlo simulation.

C. Monte Carlo simulation

It is well-known that we can write the quantum partition function of a quantum system, $Z = Tre^{-\beta\hat{H}}$ as the sum over all paths taken by the system in imaginary time defined by the scale $\hbar\beta$. If the quantum system is D-dimensional then the partition function will look like the path integral of a D+1-dimensional classical system in which the extra dimension is the time direction $0 < \tau < \beta\hbar$. At zero temperature $\beta \to \infty$ the classical system is truly D+1-dimensional. One can derive an effective Hamiltonian for such a classical system from the quantum Hamiltonian using a complete set of basis states. In this classical system the parameters of the quantum system (in our case δ) is a control knob like temperature. We can use Monte Carlo simulation of such a classical system and find out the universal behavior of the quantum system.

To develop a 1+1-dimensional classical theory for our 1D ring array we first stagger the order parameter, $\theta_i \to (-1)^i\theta_i$ so that we can analyze the Monte Carlo results easily. We also use dipole approximation for the Coulomb interaction. Consequently we can write the Hamiltonian of the system as:

$$\hat{\mathcal{H}} = \frac{E_c}{2}\sum_{j=1}^{N}(-i\frac{\partial}{\partial\theta_j})^2 - E_J\sum_{j=1}^{N}\hat{V}. \quad (9)$$

In which $E_c = \hbar^2/mR^2$ and $E_J = e^2\epsilon^2/2D$. The standard derivation[12] using the Villain approximation[13, 14] tells us that the 1+1D classical partition function equivalent to the 1D interacting quantum ring array at

zero temperature is:

$$Z \propto \int \mathcal{D}\theta(\tau) \prod_{a=1}^{\mathcal{N}} \exp\Big\{\frac{\hbar}{E_c \delta\tau} \sum_{k=1}^{N} \cos[\theta_k(\tau_{a+1}) - \theta_k(\tau_a)] + \frac{\delta\tau E_J}{\hbar} \sum_{k=1}^{N} V_k(\tau_a)\Big\}. \quad (10)$$

Where $\mathcal{D}(\theta) \equiv \prod_{a=1}^{\mathcal{N}} D\theta(\tau_a)$ and

$$V_k(\tau_a) = 3\cos[\theta_k(\tau_a) - \theta_{k+1}(\tau_a)] + \cos[\theta_k(\tau_a) + \theta_{k+1}(\tau_a)] - 3\cos[\theta_k(\tau_a) - \theta_{k+1}(\tau_a)]\cos[\theta_k(\tau_a) + \theta_{k+1}(\tau_a)]. \quad (11)$$

The parameter τ has the dimension of time and $\mathcal{N}\delta\tau = \beta\hbar$. It can be shown that the field $\theta(x,\tau)$ obeys the periodic boundary condition , $\theta(\tau + \beta\hbar) = \theta(\tau)$ ([15]). We will also assume periodic boundary condition in space direction all over the simulation.

By defining the spin vector $\vec{S}_i = (\cos\theta_i, \sin\theta_i)$ we can interpret Eq.(10) as a two dimensional classical spin model. Our early calculations suggested that the system of 1D rings has a transition from the unpolarized to the AFE state. In this classical analogue because we have already staggered the order parameter we expect to see a transition from unpolarized to ferromagnetically polarized state (FE). Close to this transition the spatial variation of the order parameter $\vec{S}$ is smooth so we can approximate (11) as follows:

$$V_k(\tau_a) \approx 3\cos(\theta_k(\tau_a) - \theta_{k+1}(\tau_a)) - 2\cos 2\theta_k(\tau_a). \quad (12)$$

Using the above potential finally the classical partition function looks like:

$$Z \propto \int \mathcal{D}\theta(\tau) \exp\Big\{K \sum_{\langle ij\rangle} \cos(\theta_i - \theta_j) - \frac{2K}{3} \sum_i \cos 2\theta_i\Big\}. \quad (13)$$

Where i and j run over an infinite 2D square lattice and we have determined $\delta\tau$ to identify the two couplings in eq.(10) as $K = \sqrt{\frac{3E_J}{E_c}}$. Equation (13) is a 2D XY model with a symmetry breaking field which is 2/3 the XY coupling. Our Monte Carlo analysis shows that this model has a continuous phase transition. The order parameter of this system is the total magnetization density equivalent to the total staggered polarization of the 1D ring array:

$$\vec{m} \equiv \langle \vec{S} \rangle \longleftrightarrow \vec{P}_s. \quad (14)$$

Where the average on the left hand side is the thermodynamic average over the infinite size lattice.

The fluctuations in this system is controlled by K which is the analogue of $1/T$ in real classical systems. We can measure the analogue of specific heat of the system using:

$$\tilde{C}_v = \frac{1}{N^2}(\langle E^2\rangle - \langle E\rangle^2) \quad (15)$$

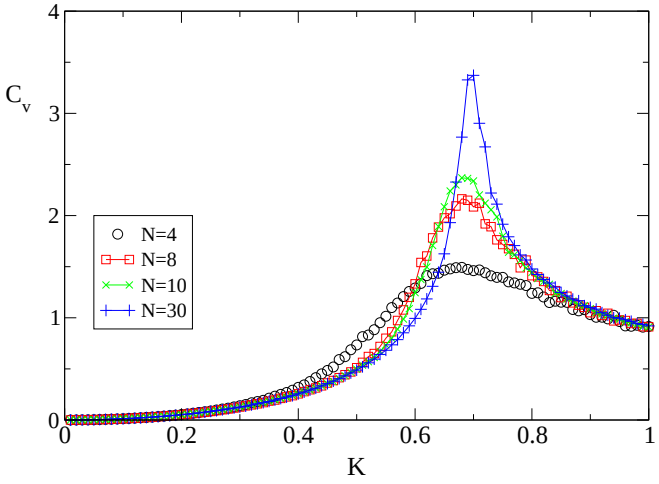

FIG. 5: Monte Carlo results of the $\tilde{C}_v = \overline{\Delta E^2}/N^2$ for different system sizes. The system is a 1+1D classical equivalent of 1D quantum ring array at zero temperature.

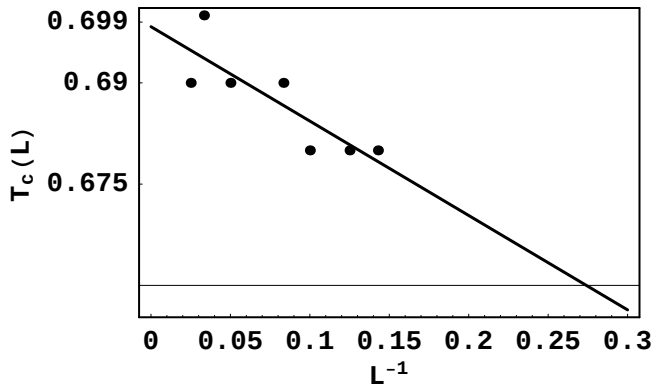

FIG. 6: Plot of critical coupling $K_c(L)$ at different system sizes taken from the C_v plots. The solid line is a linear fit to the data indicating $K_c(\infty) \approx 0.699$.

in which $\langle . \rangle$ is the average over an ensemble and E is the total energy of the $N \times N$ system. This quantity diverges at the critical point of the infinite system undergoing a continuous phase transition. Fig.(5) shows the change of the specific heat of our 1+1D system in terms of the parameter K for different lattice sizes. As we can see at K_c the peak gets sharper and sharper with increasing lattice size L. An extrapolation of the point of the maximum of C_v, $K_c(L)$ to $L^{-1} = 0$ determines the approximate critical point of the infinite lattice(Fig.6) . Also an extrapolation of $m(L,K)$ for different values of K in Fig.(7) shows that a real continues phase transition happens in the infinite size system.

The effective classical system derived here does not fully explain all the physical aspects of the 1D quantum system mainly because of the approximations used to derive the path integral. However, we believe that, close to the critical region, these approximations do not

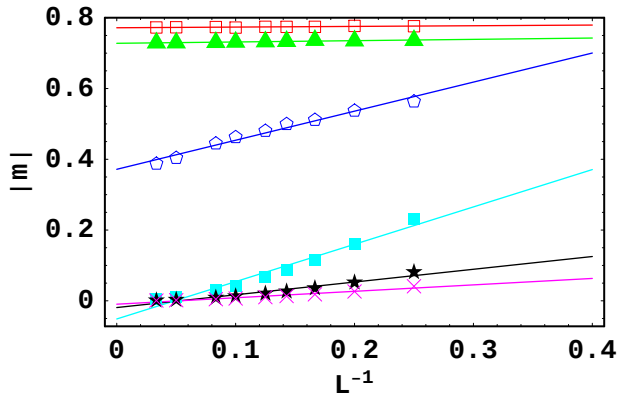

FIG. 7: Extrapolation of the total magnetization density of the 1+1D classical system to infinite size at couplings $K/K_c(\infty)$=1.45(empty boxes), 1.32(triangles), 1.03(polygons), 0.74(filled boxes), 0.45(stars) and 0.16(crosses). The solid lines are linear fit to each set of data.

play any role in the general behavior of the system and the universality class remains unchanged. Hence using the finite size scaling method we can determine the critical exponents of the classical system and determine the universality class of the actual quantum system.

1. *Finite size scaling of the 1+1D system*

One of the best parameters for examining the phase transition and find the universal exponents with finite size scaling is the dimensionless Binder ratio:

$$g_L = \frac{\langle m^4 \rangle}{\langle m^2 \rangle^2} \tag{16}$$

defined for a system with size L. In the disordered phase $K < K_c$ the correlation length ξ is finite so for $L \gg \xi$ the distribution of m is Gaussian around $m = 0$ with the width $\sim N^{-1/2} \sim L^{-d/2}$ so $g \to 0$. On the other hand for $K > K_c$ where $\langle m \rangle$ is finite, g_L approaches a constant as $L \to \infty$. The variation of g_L with K becomes sharper and sharper as L increases, however all the g's cross at the transition point K_c. The variation is given by the following finite size scaling function:

$$g_L(K) = \widetilde{g}(L^{1/\nu}(K - K_c)). \tag{17}$$

Where $\widetilde{g}$ is a scaling function which depends on L and K only in that particular form. By using the finite size data we can try to find a data collapse and by calculating the standard deviation find the best exponent ν fitting to the collapsed function. Fig(8) shows the Binder ratio for different lattice sizes. Fig.(9) shows the collapsed data and Fig.(10) shows the best exponent is $\nu = 0.99 \pm 0.01$. The error is estimated from the mesh of the numerical calculation.

The scaling for the order parameter $|m|$ is:

$$m = L^{-\beta/\nu} X^0(L^{1/\nu}(K - K_c)). \tag{18}$$

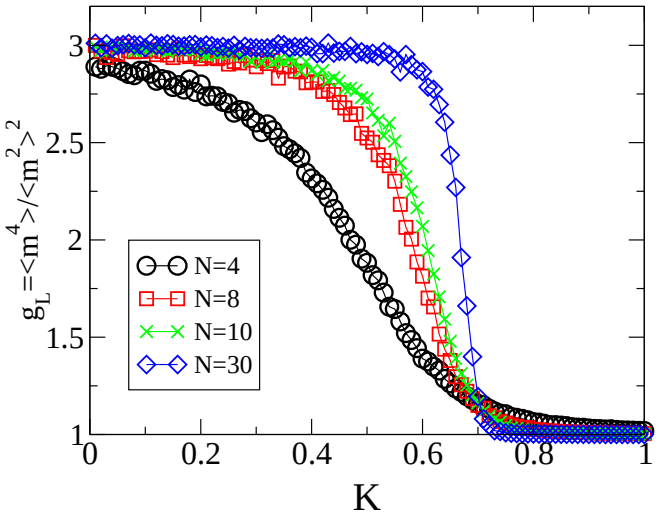

FIG. 8: Plots of Binder ratio for different system sizes. The behavior is sharper at larger sizes.

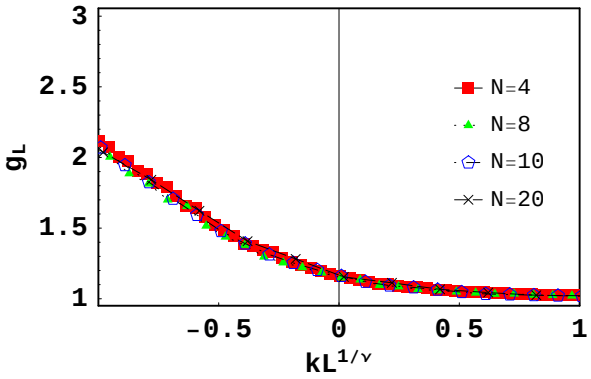

FIG. 9: Collapse of Binder plots at the critical region. The best collapse is obtained for $\nu = 1.01 \pm .01$.

Where X^0 is a function of $x = L^{1/\nu}(K - K_c)$ only and β is one of the universal scaling exponents of the system. To determine the universal exponent β we plot $L^{\beta/\nu}$ vs. x for different sizes. Fig.(12) and (13) show the the collapse of different data sets and the standard deviation for different exponents respectively which shows the best estimation is $\beta = 0.125 \pm .005$, or $1/8$.

2. *Universality Class*

The universal exponents extracted from the finite size data indicate that our 1+1D classical XY model in the symmetry breaking field is in the universality class of 2D classical Ising model, hence the nature of quantum phase transition of our 1D quantum ring array is Ising-like. The Coulomb repulsion forces the electrons to alternate staying on the top and bottom of the rings. However the quantum kinetic energy tries to avoid localization. This

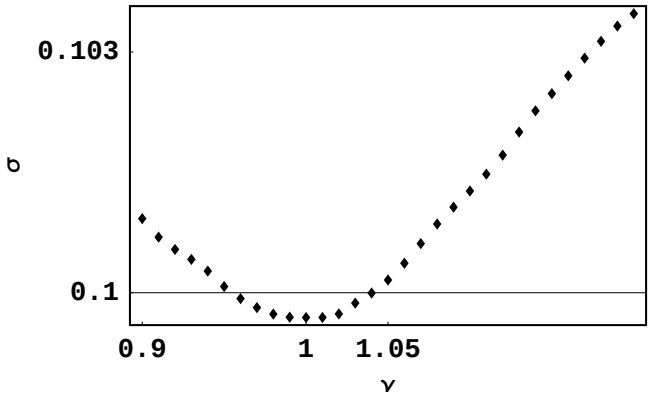

FIG. 10: Standard deviation of the set of scaled plots of Binder ratio for different exponents. The case for $\nu = 1$ is the best choice which is plotted in Fig.(9).

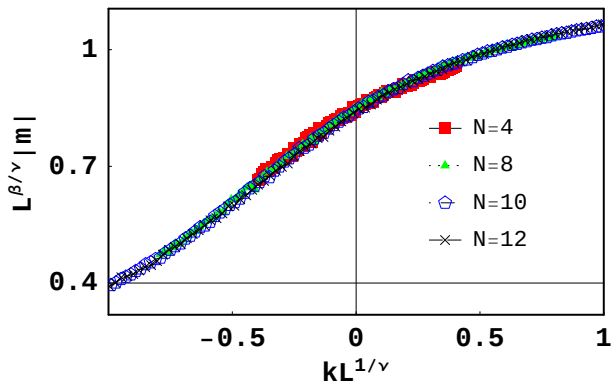

FIG. 12: Collapse of scaled magnetization data sets for $\nu = 1$ and $\beta = 1/8$ in the critical region.

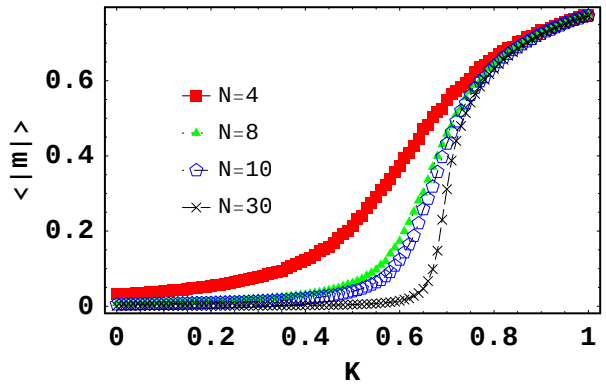

FIG. 11: Monte Carlo results of average magnetization of the 1+1D classical system for different system sizes. The change of magnetization tends to be sharper as the system size grows.

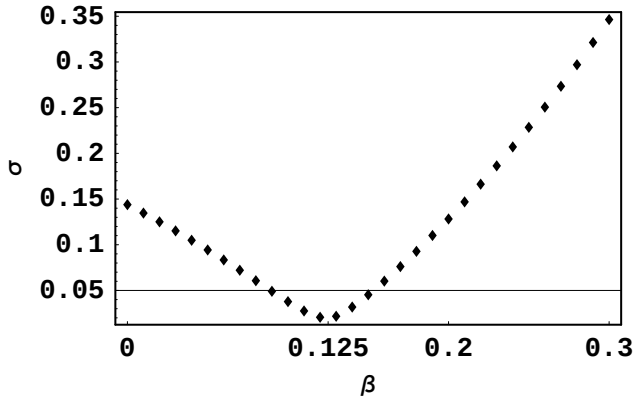

FIG. 13: Standard deviation of the set of scaled plots of magnetization for fixed $\nu = 1$ and different exponent β. The case for $\beta = 1/8$ is the best choice which is plotted in Fig.(12).

kinetic energy causes the electrons to tunnel from top into bottom of the ring hence destroying the antiferroelectric order. This ordering behavior shows up in the probability distribution on each ring. Fig.(14) shows the energy of each electron with the wavefunction $\psi_d(\theta) = x + y\cos(2\theta)$ compared to when the wavefunction is a constant all around the ring. The wavefunction ψ_d has two maxima on top and bottom of the ring which means the electron is fluctuating up and down. As we can see by increasing the coupling the lower energy state selected by the exact Hartree calculations (dots) gradually matches ψ_d instead of the constant wavefunction. This behavior persists in a range of couplings close but smaller than the critical coupling i.e. in disordered region $\delta < \delta_c$. Needless to say that after transition point the ground state wavefunction is no longer ψ_d and the system starts to excite more angular momentum eigenstates (Fourier modes).

All the above discussion suggests that the nature of the antiferroelectric transition is not just the simple 2D Ising but is similar to *1D transverse field Ising*(TFI) which has a quantum phase transition at zero temperature in

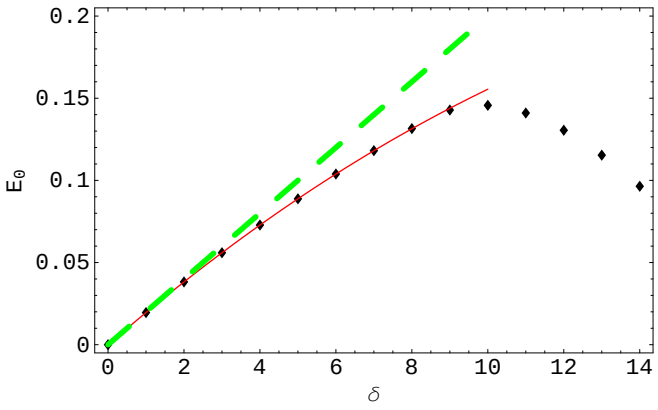

FIG. 14: Plot of the energy of interacting quantum ring array when all the wavefunctions are constant around the ring (dashed) or all are in the form of $\psi_d = a + b\cos 2\theta$(solid). The points are the actual results coming out of the numerical Hartree calculation indicating that ψ_d is the selected behavior for $\delta < \delta_c \approx 8$.

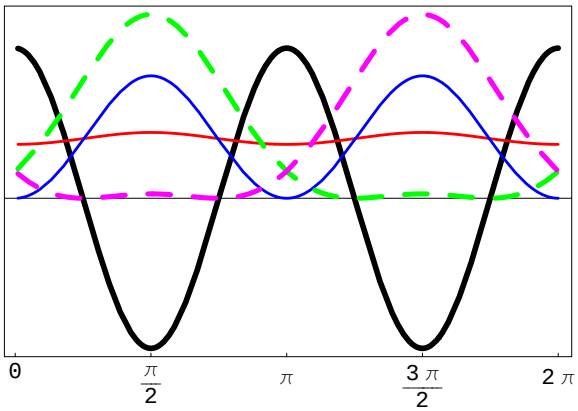

FIG. 15: Plot of the $\cos 2\theta$ potential around a ring (the thick solid line), the ground and first excited state of this potential (thin solid lines) coming out of a simple numerical Schrodinger equation solver and the up and down states (dashed lines) constructed from the two eigenstates(see appendix). The scale of the potential is exaggerated for easier comparison.

the same universality class as 2D Ising. We can develop an effective 1D TFI hamiltonian for our ring array in the dipole approximation. In this approximation we can write down the hamiltonian(9) as follows :

$$\begin{aligned}\hat{H} &= \hat{H}_0 + \hat{V} \\ \hat{H}_0 &= \sum_i \left[(-i\frac{\partial}{\partial\theta_i})^2 + 3\delta\epsilon^2\cos 2\theta_i\right] \\ \hat{V} &= -\delta\epsilon^2 \sum_i \left[3\cos(\theta_i+\theta_{i+1}) + \cos(\theta_i-\theta_{i+1})\right].\end{aligned} \tag{19}$$

The $\cos 2\theta$ term in hamiltonian $\hat{H}_0$ has two minima at top and bottom of the ring. Fig.(15) shows the potential and the two lowest energy states of it with energies $E_0 < E_1$. The rate of tunnelling from top to bottom or vice versa is determined by $\Delta \equiv E_1 - E_0$. The potential $\hat{V}$ tries to align the electrons hence it acts like the Ising interaction. A more rigorous derivation using the Holstein-Primakov bosons[16] shows that the projection of the hamiltonian $\mathcal{H}$ into the subspace of the ground and first excited states of $\hat{H}_0$ can be written as (see appendix):

$$\hat{H} \approx \Delta \sum_{i=1}^{N} \sigma_i^x - J\sum_{i=1}^{N}\sigma_i^z\sigma_{i+1}^z. \tag{20}$$

In which σ's are Pauli spin matrices and $J = 8\delta\epsilon^2$. Numerical diagonalization of $\hat{H}_0$ tells us that $\Delta \approx 1 - 0.1\delta\epsilon^2$ for small ϵ.

Close to transition the Coulomb repulsion is not strong enough to excite the electrons to higher states, consequently the TFI model in Eq.(20) is valid and indicated the nature of transition of the 1D ring array.

V. QUANTUM RINGS TRANSITIONS FOR $B \neq 0$

Y. Aharanov and D. Bohm (AB) have predicted that the wavefunction of an electron moving in a vector potential $\vec{A}(x)$ along the path C acquires a phase shift:

$$\Delta\Lambda = \frac{e}{\hbar c}\int_C \vec{A}\cdot\vec{dr}. \tag{21}$$

AB predicted that this phase shift can be observable. When an electron is confined on a closed path like the case of charged ring threaded by magnetic flux ϕ the phase shift after one 2π rotation would be :

$$\Delta\Lambda = \frac{e}{\hbar c}\oint \vec{A}\cdot\vec{dr} = \phi/\phi_0. \tag{22}$$

Where $\phi_0 = hc/e \simeq 4.135\times 10^{-7} G.cm^2$ is the quantum of flux. The phase shift above has been observed in numerous experiments and different devices including the experiments of persistent current and excitons in quantum rings. In this section we show how magnetic field changes the behavior of polarization.

The Hamiltonian of an electron in 1D a ring threaded by a constant uniform magnetic field $B\hat{z}$ (the ring is in the x-y plane) is:

$$\hat{H} = \frac{\hbar^2}{2mR^2}(i\frac{\partial}{\partial\theta} + \frac{\phi}{\phi_0}) \tag{23}$$

in which the choice of gauge: $\vec{A} = \frac{B}{2}(-y, x, 0)$, the momentum is in polar coordinates:$\hat{p} = -i\frac{\hbar}{R}\frac{\partial}{\partial\theta}$ and the eigenfunctions are periodic: $\psi(\theta + 2\pi) = \psi(\theta)$. The eigenenergies of (23) will be:

$$E_n = \frac{\hbar^2}{2mR^2}(n - \phi/\phi_0)^2 \tag{24}$$

in which n is an integer. By changing the gauge $\vec{A} \to \vec{A} - \nabla\Lambda$ wavefunctions undergo a phase change $\psi \to e^{\frac{ie}{\hbar c}\Lambda}\psi$. For example we can use the gauge transformation with the choice of $\Lambda = (BR^2/2)\theta$ to remove the vector potential from (23) but at the same time we have to shift the phase of the wavefunctions to $e^{-i\frac{\phi}{\phi_0}\theta}\psi$. As the result the eigenfunctions change:

$$\psi_n(\theta) = \frac{1}{\sqrt{2\pi}}e^{i(n-\phi/\phi_0)\theta}. \tag{25}$$

This eigenfunction however has a different boundary condition than the previous one :

$$\psi(\theta + 2\pi) = e^{2\pi i\phi/\phi_0}\psi(\theta) \tag{26}$$

but as one physically expects the eigenenergies are not changed. The ground state energy of the interacting

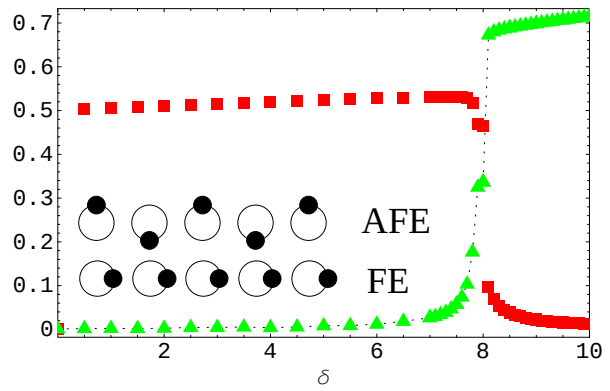

FIG. 16: Results of numerical Hartree calculations of the polarization of a 1D quantum ring array threaded by half-flux quantum $\phi/\phi_0 = 1/2$. For $\delta < \delta_c$ the system displays a longitudinal ferroelectric (FE) polarization (squares), while for $\delta > \delta_c$ an antiferroelectric (AFE) polarization (triangles) is observed.

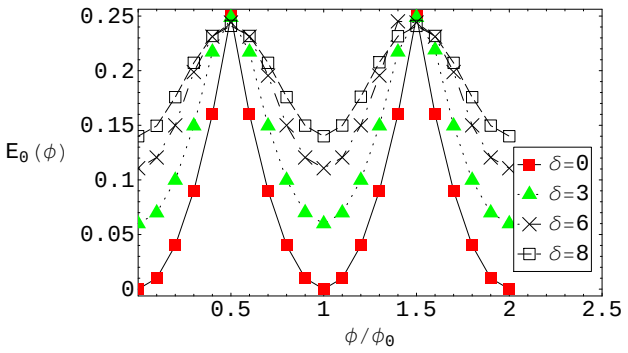

FIG. 17: Plots of ground state energy of the interacting quantum ring array in the external magnetic flux threading each ring for different couplings δ. The physics is periodic because of Aharanov-Bohm induced phase that is proportional to the flux.

quantum ring array in the magnetic flux ϕ can be written as:

$$E_0(\delta,\phi) = \sum_{n=-n_0}^{n_0} |c_n|^2 (n-\phi/\phi_0)^2 + \\ + \delta \sum_{\langle ij\rangle} \int d\theta d\theta' \frac{|\Psi_0(\theta)|^2 |\Psi_0(\theta')|^2}{|\vec{r}_i(\theta) - \vec{r}_j(\theta')|} \quad (27)$$

where $\Psi_0(\theta) = e^{i\phi/\phi_0\theta} \sum_{n=-n_0}^{n_0} c_n e^{in\theta}$ is the ground state wavefunction expanded in the free hamiltonian basis states. As we can see in Eq.(27) the only part that is affected by the AB phase is the kinetic energy and the potential energy is not sensitive to the phase. The energy calculated in Eq.(27) is periodic in ϕ_0 since when $\phi = \phi_0 = 1$ we can rearrange the infinite sum and show that the value of the kinetic energy is equal to its value at

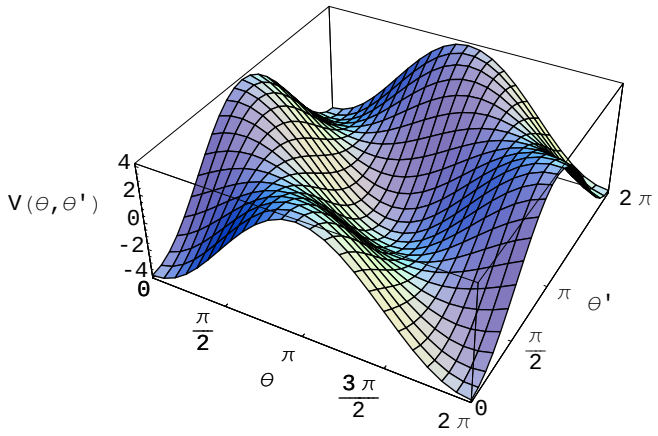

FIG. 18: Plot of the two-body potential function in Eq.28. The interacting rings in magnetic field select the minimum of this potential for their ground state wavefunction at low couplings. The potential is in units of $\delta\epsilon^2$.

$\phi = 0$. This is due to the well-known fact that the physics of quantum rings does not change at integer flux quanta. For infinite n_0 this argument is true at any range of magnetic flux; in our numerical calculations where we have used a finite number of Fourier modes E_0 is periodic only in a finite range approximately given by $0 < \phi < n_0\phi_0$ in Fig.(17) we can see the periodic behavior of the ground state energy of the ring array as magnetic flux changes.

The results of our numerical Hartree calculations indicate that in a 1D ring array in which each ring is threaded by a magnetic flux ϕ the polarization pattern changes from unpolarized to ferroelectric at half-integer flux quantum. Fig.(16) shows the behavior of P_x , the component of the total polarization vector $\vec{P} = \sum_i \int_0^{2\pi} d\theta |\psi_i(\theta)|^2 \vec{r}_i(\theta)$ in the direction of the ring's common axis at half flux quantum. This plot shows that at $\delta < \delta_c$ the wavefunction has an unbalanced distribution around each ring. However the total polarization vanishes at higher values of interaction where the wavefunction distribution becomes antiferroelectrially polarized in the array. The finite polarization at small interaction strengths has a ferroelectric pattern which is degenerate left or right. From this result we can see that the physics of quantum ring arrays changes at half integer flux quantum. The total staggered polarization in the $\hat{y}$ direction perpendicular to the common axis of the rings starts to build up at $\delta > \delta_c$ as in the case of no magnetic field. We can explain this phenomena of *finite transverse polarization due to magnetic field* in different approaches.

We can use a simple perturbative discussion to understand this behavior qualitatively. The Eq.(19) which is the dipole approximation of the total hamiltonian will

modify in presence of a magnetic flux as follows:

$$\begin{aligned}\hat{H} &= \hat{H}_0 + \hat{V} \\ \hat{H}_0 &= \sum_i \left[(-i\frac{\partial}{\partial\theta_i} - \frac{\phi}{\phi_0})^2 + 3\delta\epsilon^2\cos 2\theta_i\right] \\ \hat{V} &= -\delta\epsilon^2 \sum_i \left[3\cos(\theta_i + \theta_{i+1}) + \cos(\theta_i - \theta_{i+1})\right].\end{aligned} \tag{28}$$

In the above equation the kinetic energy hamiltonian has a degenerate ground state. For example at half filling, $\phi/\phi_0 = \frac{1}{2}$, $n = 0$ and $n = 1$ levels are degenerate unlike the case of zero magnetic field in which the ground state is unique and at $n = 0$. By adding the symmetry breaking term $\cos 2\theta$ in the zero flux the electron gains enough energy to excite to the next higher level. This excitation causes the electron to destroy any localization in the range where $\hat{V}$ is not strong enough yet. However when there is a finite magnetic field the $\cos 2\theta$ can not lift the degeneracy between $n = 0$ and $n = 1$ levels in the range of small δ's. That is why in this case the ground state of $\hat{H}_0$ remains degenerate(Fig.17). As long as δ is small the perturbative two body potential in (28) can not excite the electron to higher levels and the kinetic energy of the electron freezes. When this happens the electrons behave classicaly and choose a wavefunction that minimizes the potential $\hat{V}$. In Fig.(18) we can see a 3D plot of the two body potential V in which it has two stable minima at (π, π) and $(0, 0)$ indicating the preferred state of the quantum ring array at low δ being the ferreoelectric right or left state.

It is surprising that the system orders ferroelectricallly along the chains. This occurs because the charge distribution is quite broad. Using only the two lowest Fourier modes the charge distribution can be written in general as $\rho(\theta) = (1 + \cos(\theta - \theta_0))/2\pi$, which nearly wraps around the ring. If we change this to an (unphysical) flat charge distribution with an artificially varying width, the FE state has a lower energy than the AFE state when the width $\Delta\theta \sim .45\pi$, while for a triangular distribution the FE distribution is favored when $\Delta\theta \sim 0.6\pi$. While the exact transition depends of course upon ϵ, these calculations help explain why the FE phase wins out at half filling.

VI. CONCLUSIONS

In this paper we have shown that there is a phase transition in a periodic array of electrons each confined to a 1D ring. The parameter δ determines if the array will spontaneously polarize; in 1D the transition is at $\delta \approx 10$. It is easy to achieve small values of δ simply by choosing the ring separation to be large. Thus the "quantum" limit where the kinetic energy dominates is simple to obtain. To obtain the antiferroelectrically ordered state we need large δ. We may write this as $\delta = (R^2/a_0 D) \times (m^*/m)$ where a_0 is the Bohr radius and m^* is the effective mass of the electron. If $\tilde{R}$ and $\tilde{D}$ are R and D measured in nanometers, and $\tilde{m} \equiv (m^*/m)$, then $\delta \approx 18.9(\tilde{R}^2/\tilde{D})\tilde{m}$. We require that the rings do not intersect, so that $\tilde{D} \geq 2\tilde{R}$. Thus the ability to achieve large values of δ in semiconductors will depend upon the value of the effective mass. If we set $\tilde{D} = 2\tilde{R}$, then for GaAs ($\tilde{m} = 0.06$) 1D arrays of rings with a radius greater than ∼10nm will be polarized. For AlAs ($\tilde{m} = 0.4$) the crossover radius is about 70nm. Rings with a smaller radius will not spontaneously polarize, but instead be isotropic

It is well known that in 1D there is no ordered state for $T > 0$ for the Ising model. However, for small arrays over finite time intervals the system can order. To observe this behavior we want the characteristic energies of the system to be greater than the temperature. For the Coulomb energy $kT < e^2/D$, which we may write as $\tilde{D}T < 1.8 \times 10^3$ where T is in Kelvin. For the kinetic energy this means $kT < \hbar/2m^*R^2$; if we measure $(m/m^*)\tilde{R}^2T > 40$ in the same units. For GaAs we can choose R to be about 14nm at 4K; choosing materials with a smaller effective mass or going to lower temperature allows us to increase the radius.

An AFE polarized ring array will scatter light at a wavelength commensurate with the inter-ring separation, D. In 1D there is a gap $\sqrt{2}\omega_0$, which we may write as $2\sqrt{2\tilde{m}}(a_0/D)^{3/2}$. For GaAs rings with a separation $D = 1000$nm this gives $\omega \sim 6.0 \times 10^{10}$Hz. The 2D arrays have a similar sized gap at zone center, but the gap vanishes at one zone edge. The excitation spectrum can be probed optically, but scattering at the edge of the zone is difficult due to the constraints imposed by conservation of energy and momentum. Typically in such cases Raman scattering can be used to investigate the excitations.

While we have not explicitly addressed the 2D case here, much can be gleaned from our results. The 2D classical problem obviously has a finite temperature phase transition, as shown by our Monte Carlo simulations. The 2D quantum problem can be mapped on to the 3D XY model, which is known to order. We have performed simulations on the 2D case and find that it orders in a striped phase.[17]

Finally these calculations assume that each ring is singly occupied. This might be obtained by fabricating the rings upon a thin insulating layer covering a gate. By tuning the gate voltage we can bias the system so that it is energetically favorable for an electron to tunnel to the rings. The gate will also serve to cutoff long distance interactions between the rings, supporting the assumption of the nearest neighbor interactions used here. Moreover, this letter serves to start investigation into a broad class of problems, such as rings occupied by an optically excited exciton/hole pair or perhaps by a small, varying number of electrons created by a random distribution of dopants.

The topic of quantum dot arrays and their correlations has obvious and useful analogies with solid state models

of crystalline arrays of atoms. In this paper we wish to point out that experimentalists have at their disposal a host of "unnatural atoms" analogs: rings, quantum dot quantum wells, quantum rice, etc. The electrons in these nanoscale constituents are confined to orbitals that may not have atomic analogs. Morever, it may be possible to tune the shape of the constiutent to optimize some desired collective property such as frustration in electric or magnetic polarization, high susceptibility or sensitivity to optical polarization of light. Even more rich behavior will develop if we allow electrons to tunnel between these nanoscale periodic structures.

Acknowledgments

The authors wish to thank Steve Girvin, Herbert Fertig, and Matthew Johnson for several useful discussions. This work is supported by NSF MRSEC DMR-0080054 (BR), and NSF EPS-9720651 (KM).

APPENDIX: TRANSVERSE FIELD ISING MODEL

In this section we explain how one can write the projection of the hamiltonian (19) into ground and first excited state subspace of $\hat{H}_0$ as a 1D transverse field Ising model (Eq.20). In order to make the analysis easier we change the variables θ_i to staggered one, $(-1)^i\theta_i$. Defining $|0\rangle$ and $|1\rangle$ as ground and first excited states of $\hat{H}_0$ and E_0 and E_1 the corresponding eigenenergies we can write the up and down states (Fig.15) as:

$$\begin{aligned} |\uparrow\rangle &= \frac{1}{\sqrt{2}}(|0\rangle + |1\rangle) \\ |\downarrow\rangle &= \frac{1}{\sqrt{2}}(|1\rangle - |0\rangle). \end{aligned} \tag{A.1}$$

Now we define the creation and annihilation operators:

$$\begin{aligned} c_\uparrow^\dagger|\uparrow\rangle &= c_\downarrow^\dagger|\downarrow\rangle = 0 \\ c_\uparrow^\dagger|\downarrow\rangle = |\uparrow\rangle \quad &, \quad c_\downarrow^\dagger|\uparrow\rangle = |\downarrow\rangle, \end{aligned} \tag{A.2}$$

and one can show that :

$$[c_\alpha, c_\beta^\dagger] = \delta_{\alpha\beta}. \tag{A.3}$$

So we can write the hamiltonian (19) as:

$$\hat{H} = \sum_{i=1}^{N} \sum_{\alpha,\beta=\uparrow,\downarrow} \varepsilon_{\alpha\beta} c_{i\alpha}^\dagger c_{i\beta} + \sum_{\langle ij\rangle} \sum_{klmn=\uparrow,\downarrow} V_{klmn}^{ij} c_{ik}^\dagger c_{jm}^\dagger c_{jn} c_{li}, \tag{A.4}$$

in which i, j are spatial indices and:

$$\varepsilon = \frac{1}{2}\begin{pmatrix} \varepsilon_0 & \Delta \\ \Delta & \varepsilon_0 \end{pmatrix} \tag{A.5}$$

where $\varepsilon_0 = E_1 + E_0$ and $\Delta = E_1 - E_0$. To calculate matrix elements of the potential we use a simple numerical Schrodinger equation solver to find the following quantities:

$$\begin{aligned} \langle\uparrow|\cos\theta|\uparrow\rangle &= \langle\downarrow|\cos\theta|\downarrow\rangle \approx 0 \\ \langle\uparrow|\cos\theta|\downarrow\rangle &= \langle\downarrow|\cos\theta|\uparrow\rangle \approx 0 \\ \langle\uparrow|\sin\theta|\uparrow\rangle \approx +1 \quad &, \quad \langle\downarrow|\sin\theta|\downarrow\rangle \approx \\ \langle\uparrow|\sin\theta|\downarrow\rangle &= \langle\downarrow|\sin\theta|\uparrow\rangle \approx 0 \end{aligned} \tag{A.6}$$

In the above diagonal matrix elements of $\cos\theta$ are approximately zero because must of the wavefunction is localized around $\theta = \pm\pi/2$. For the same reason the diagonal matrix elements of $\sin\theta$ are ± 1. Using the above we can derive the potential in the following second quantized form:

$$\begin{aligned} \hat{V} &= -2\delta\epsilon^2 \sum_{\langle ij\rangle} (c_{i\uparrow}^\dagger c_{j\uparrow}^\dagger c_{j\uparrow} c_{i\uparrow} - c_{i\uparrow}^\dagger c_{j\downarrow}^\dagger c_{j\downarrow} c_{i\uparrow} + \\ &- c_{i\downarrow}^\dagger c_{j\uparrow}^\dagger c_{j\uparrow} c_{i\downarrow} + c_{i\downarrow}^\dagger c_{j\downarrow}^\dagger c_{j\downarrow} c_{i\downarrow}). \end{aligned} \tag{A.7}$$

Now we can use the Holstein-Primakov transformation [16] to construct the following SU(2) covariant operators for each lattice point:

$$S^+ = c_\uparrow^\dagger c_\downarrow \ , \ S^- = c_\downarrow^\dagger c_\uparrow \ , \ S^z = \frac{1}{2}(c_\uparrow^\dagger c_\uparrow - c_\downarrow^\dagger c_\downarrow). \tag{A.8}$$

Using the above definitions and the fact that: $c_\uparrow^\dagger c_\uparrow + c_\downarrow^\dagger c_\downarrow = 1$ for each lattice point we arrive at the following expression for the hamiltonian (19):

$$\hat{H} = -8\delta\epsilon^2 \sum_{i=1}^{N} S_i^z S_{i+1}^z + \Delta \sum_{i=1}^{N} S_i^x, \tag{A.9}$$

in which: $S^{x,y} = (S^+ \pm iS^-)/2$.

[1] *Quantum Wells, Wires and Dots : Theoretical and Computational Physics of Semiconductor Nanostructures*, Paul Harrison (John Wiley & Sons, New York, 2005).
[2] A. Lorke et. al., Phys. Rev. Lett., **84**, 2223(2000)
[3] K. L. Hobbs, P. R. Larson, G. D. Lian, J. C. Keay, and M. B. Johnson, Nano Lett., **4**, 167 (2004).
[4] M. Büttiker, Y. Imry and R. Landauer,Phys. Lett. A, **96**, 365 (1983)
[5] R. Landauer and M. Buttiker, Phys. Rev. Lett., **54**,2049(1985)
[6] L. P. Levy, G. Dolan, J. Dunsmuir and H. Bouchiat, Phys. Rev. Lett.,**64**,2074 (1990), V. Chandrasekhar et. al., Phys. Rev. Lett.,**67**,3578(1991)
[7] S. Tarucha, D. G. Austing, T. Honda, R. J. vanderHage

and L. P. Kouwenhoven, Phys. Rev. Lett., **77**,3613 (1996)
[8] K. Mullen, D. Loss, and H. T. C. Stoof, Phys. Rev. B **47** 2689 (1993).
[9] The Coulomb interaction scales inversely with distance, whereas the tunneling is exponentially suppressed. Indeed it would be experimentally difficult to achieve the limit where electrons *can* tunnel between rings. In the limit where electrons can tunnel from ring to ring the dynamics are much richer (*unpublished*).
[10] *Quantum Theory of Many-Particle Systems*, A. Fetter and J. D. Walecka, (McGraw-Hill, New York, 1971).
[11] *Quantum Phase Transitions,* Subdir Sachdev (Cambridge University Press, New York, 1999).
[12] Mats Wallin and S. M. Girvin Phys. Rev. B 47, 14642 (1993).
[13] J. Villain, J. Phys. (Paris) 36, 581 (1975).
[14] J. V. Jose, L. P. Kadanoff, S. Kirkpatrick, and D. R. Nelson, Phys. Rev. B 16, 1217 (1977).
[15] Mats Wallin, Erik S. Sorensen, S. M. Girvin, and A. P. Young, Phys. Rev. B 49, 12115 (1994).
[16] Assa Auerbach, *Interacting electrons and quantum magnetism*(Springer-Verlag, New York, 1994)
[17] B. Roostaei, Kieran Mullen *unpublished*.